Reproduction of Gloss Unevenness on Printed Paper by Reflection Model with Consideration of Mesoscopic Facet

Rui Takano 1), Kaori Baba 1), Shinichi Inoue 2), Kimiyoshi Miyata 3), Norimichi Tsumura 1)
1) Graduate School of Advanced Integration Science, Chiba University, CHIBA, JAPAN
2) Mitsubishi Paper Milles Limited, TOKYO, JAPAN
3) Research Department, National Museum of Japanese History, CHIBA, JAPAN

Figure 1. *Classifying paper surface into three types of facet*

Abstract

Gloss is one of the important factors in quality of printed paper. Gloss unevenness occurring on the paper surface affects to evaluate the quality, and it is difficult to be reproduced by the Torrance-Sparrow model because the model considers only macroscopic and microscopic facets. In this paper, we reproduce the gloss unevenness on the paper surface by expanding the Torrance-Sparrow model to consider mesoscopic facets. Normal vectors of the mesoscopic facets on the paper surface were measured, and the gloss unevenness was reproduced by generating the same probability distribution to the measured distribution of the normal vectors. As a result, we could reproduce the gloss unevenness by the expanded Torrance-Sparrow model.

Introduction

Gloss is one of the important factors to evaluate quality of printed paper. The gloss is a specular reflection phenomenon that is observed at viewing angle equal to lighting angle. Surrounding scene of the observation is reflected on paper surface clearly as quality of glossy paper. Measurement technologies have been developed and reported to evaluate the gloss [1-3]. Conventionally, the gloss is evaluated as an averaged behavior on the paper surface. Typical evaluation method is standardized as using the gloss in JIS (Japanese Industrial Standards). Inoue *et al*. have measured point spread function (PSF) for the specular reflection, and showed that the PSF is helpful to evaluate gloss in the printed paper [1]. Practically, the gloss on the paper surface is not evenness. Fujiwara *et al*. reported on the measurement and analysis of the gloss [2]. Inoue *et al*. built a simple experimental setup to measure intensity distribution of reflected light on the paper surface, and analyzed the gloss unevenness in printed paper with various gloss levels [1, 3]. Although reflected light has its peak at the specular reflection angle, strong reflection is also observed around the specular reflection because the reflected light is varied with change of the lighting angle and viewing angle. This can be referred to as one of the reasons of the gloss unevenness.

Reflective paper surface can be classified into three types of facet as shown in Fig. 1. Macroscopic facet represents the shape of the paper surface. On the other hand, microscopic facet represents roughness of the paper surface that the human visual system cannot perceive. Mesoscopic facet is an intermediate between the macroscopic and microscopic facet. We consider that the gloss unevenness is caused by the mesoscopic facets that the Torrance-Sparrow model [6] does not employ. Therefore, the mesoscopic
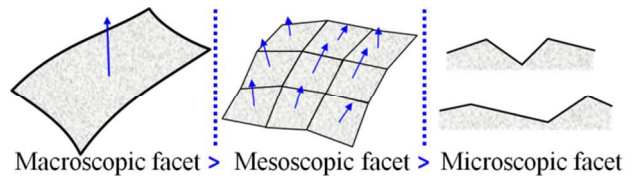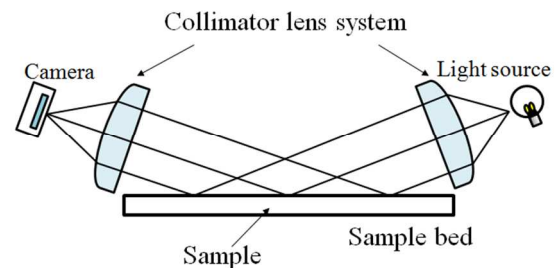

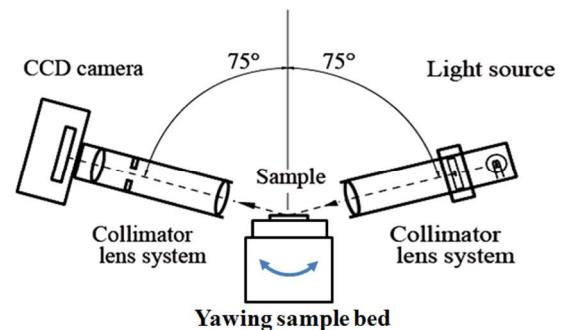**Figure 2.** *Collimator optical system*

Figure 3. *Optical setup of collimator lens system*
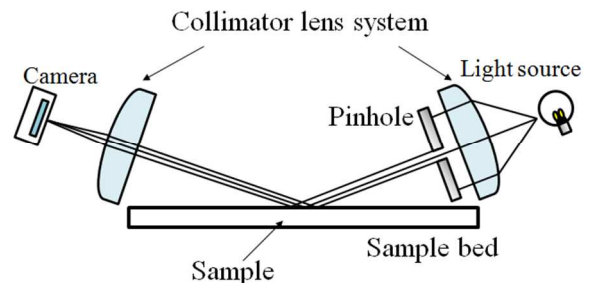

Figure 4. *Collimator optical system with masked aperture*

facet on the printed paper is introduced as an expansion of the Torrance-Sparrow model to reproduce the gloss unevenness. In this research, it is assumed that the gloss unevenness can be expressed by fluctuation of the normal vectors for the mesoscopic facets to generate random numbers based on actual measurements.

Measuring distribution of normal vectors for mesoscopic facets

Outline of collimator optical system

Light from point light source is collimated as parallel light by an optical system as shown in Fig. 2. The parallel light reflected on the paper surface is inversely collimated as an image showing the PSF of the paper surface. The PSF can be used as roughness in the Torrance-Sparrow model, since distribution of the PSF is related to angle of microscopic facets. For example, if the paper surface is rough, the PSF will be a broad distribution due to a wide range fluctuation in the angle of the microscopic facets.

Figure 3 shows the optical setup of the collimator lens system used in the experiments. The lighting and viewing angles are set to be 75 degrees according to the measuring method for specular gloss of the paper standardized by ISO [10].

Collimator lens system with pinhole aperture

As shown in Figure 4, a pinhole aperture is inserted in front of the collimator lens system to measure the PSF of paper sample. Peak value of the PSF is related to direction of the normal vectors of the mesoscopic facets.

Figure 5 is a photograph of the experimental system. The x-y stage is attached on the sample bed. This stage moves the sample two dimensionally to obtain the PSFs for the mesoscopic facets. In this experimental system, the LED lamp is used as the light source, and it is mounted at the back of the chart holder. The point light source is obtained by putting the pinhole at the chart holder. The pinhole is made of a metal plate, and its diameter is 200 μm. The CCD camera has 512x512 pixels resolution, and it yields 16 bits output levels per pixel linear to the light intensity. The paper sample is set on the sample bed, and the PSF is measured in the darkroom. We prepared a black glass, which refractive index is 1.567, as a standard.

Obtained distribution of normal vectors for the mesoscopic facets

The parallel light of 200 μm diameter illuminates a coated paper, and the normal vectors of mesoscopic facets is measured by variation of the highest output value in the pixel position. By moving the x-y stage, the normal vectors for 25×25 mesoscopic facets are measured per 200 μm as shown in Fig. 6. In this paper, we define a set of 25×25 facets as measured-size facets.

Figure 7 visualizes the distribution of the normal vectors for the measured-size mesoscopic facets, which is converted from *xyz* coordinates into RGB color values. The blue color in the figure means that the direction of the normal vector is $(x, y, z) = (0, 0, 1)$. In Figure 7, the R and G values are multiplied by 100 times to improve the visualization of the unevenness of the normal vectors. We can see that the distribution of the normal vectors is not homogenous because Fig. 7 doesn't show only in the blue color.
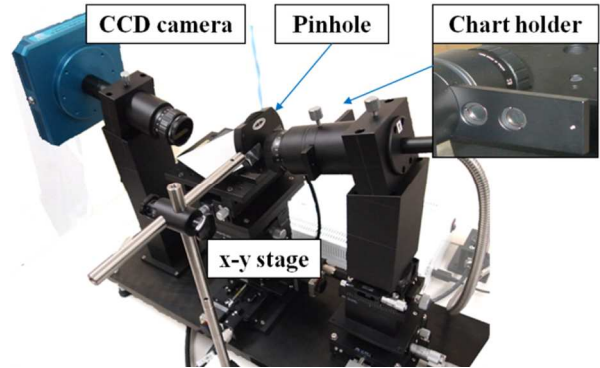

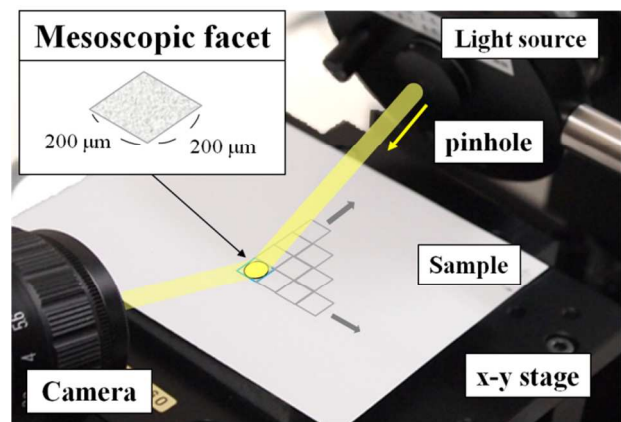**Figure 5.** Photograph showing measurement system for normal vector of mesoscopic facet.

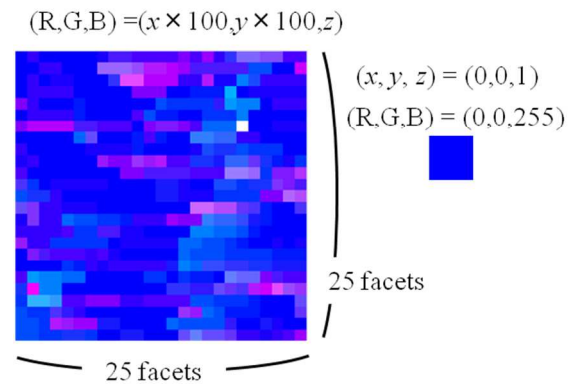**Figure 6.** Measurement for mesoscopic facet per 200 μm.

Figure 7. Visualized distribution of normal vectors in measured-size facets converted from xyz coordinates into RGB values.

Rendering by reflection model with consideration of mesoscopic facets

Conventional result by original Torrance-Sparrow model

The Torrance-Sparrow model assumed that rough surface is constructed from the microscopic facets and each facet reflects

light as a mirror. The roughness of the surface is defined by probability distribution of angles of the microscopic facets. The Torrance-Sparrow model can express phenomenon where the peak of a surface reflection shifts from the mirror reflection. The geometry of the lighting and viewing in the Torrance-Sparrow model is shown in Fig. 8. Angle θ_{in}, θ_{out}, and θ_h is the angle of incident, reflection, and between the half vector and light source direction. Angle θ_α is the angle between the half vector and normal vector. The half vector h is a vector in the position which bisects the angle which the vector l of a light-source direction and the vector e of viewing direction, and it is given a definition as follows.

$$h = \frac{l+e}{|l+e|} \ . \tag{1}$$

In the geometry shown in Fig. 8, the surface reflectance is denoted by the following equation.

$$
\begin{aligned}
&R_{s,\lambda}\left(\theta_{in},\theta_{out},\theta_h,\theta_a\right) \\
&= r_{s,\lambda} \frac{G\left(\theta_{in},\theta_{out},\theta_h,\theta_a\right)F\left(n,\theta_h\right)}{\cos\theta_{in}\cos\theta_{out}} \exp\left(-\frac{\theta_a^2}{2\sigma}\right)
\end{aligned} \tag{2}
$$

where $R_{s,\lambda}$ denotes the specular reflectance, $r_{s,\lambda}$ is the specular intensity, σ is the roughness, G is the geometrical attenuation factor that defines interception of light by asperity on the surface, and n is the relative index of refraction. $G(\theta_{in},\ \theta_{out,}\ \theta_h,\ \theta_a)$ is denoted by the following equation.

$$
\begin{aligned}
&G\left(\theta_{in},\theta_{out},\theta_h,\theta_a\right) \\
&= \min\left(1,\min\left(\frac{2\cos\theta_a\cos\theta_{out}}{\cos\theta_h}, \frac{2\cos\theta_a\cos\theta_{in}}{\cos\theta_h}\right)\right).
\end{aligned} \tag{3}
$$

The reflective coefficient of Fresnel $F(n,\theta_h)$ is denoted by the following equation by considering as $c=\cos\theta_h$, $g=\sqrt{n^2+c^2-1}$.

$$F\left(n,\theta_h\right) = \frac{1}{2}\frac{(g-c)^2}{(g+c)^2}\left(1 + \frac{(c(g+c)-1)^2}{(c(g-c)+1)^2}\right). \tag{4}$$

Figure 9 shows the result of the gloss reproduction used by computer graphics system which is OpenGL Shading Language (GLSL). The GLSL has been designed to allow application programmers to express the processing that occurs at those programmable points of the OpenGL pipeline. We reproduced the gloss according to the lighting angle where the Torrance-Sparrow model was introduced to the reflection model [4]. In Fig. 9, all of the normal vectors are evenness, therefore the gloss unevenness doesn't occur.
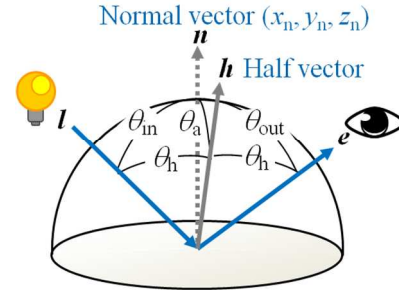

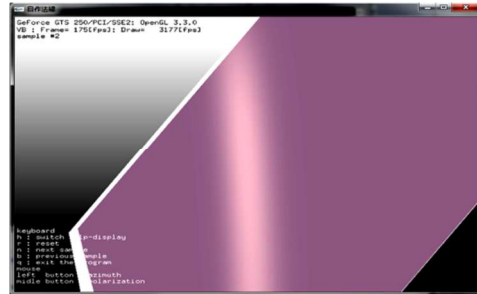**Figure 8.** Lighting and viewing geometry in the Torrance-Sparrow model
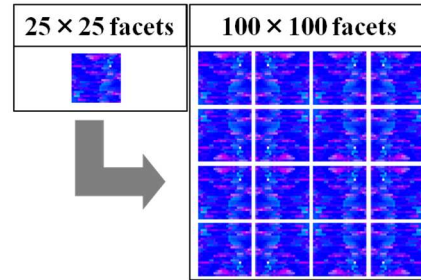

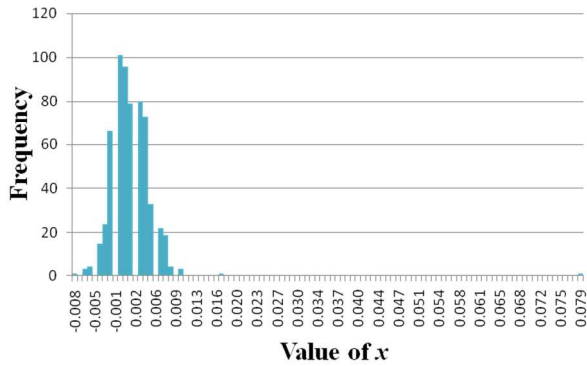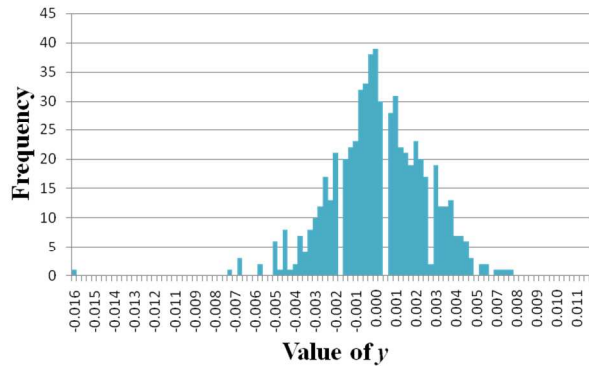**Figure 9.** Result of gloss reproduction used by GLSL

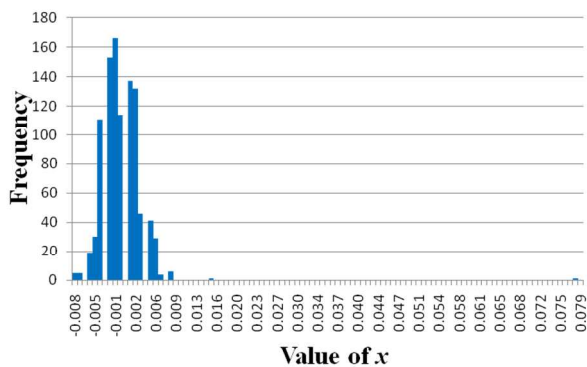**Figure 10.** Normal vector distribution consists of measured-size normal vectors distribution of 4 × 4

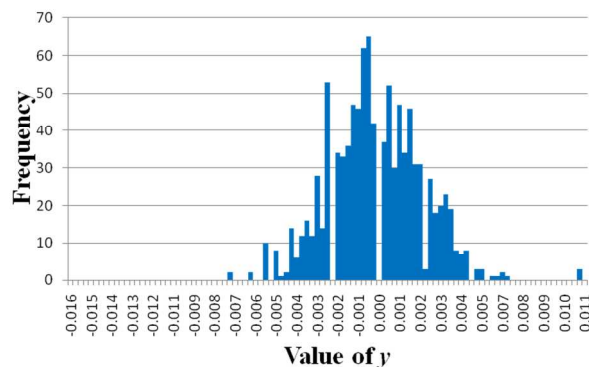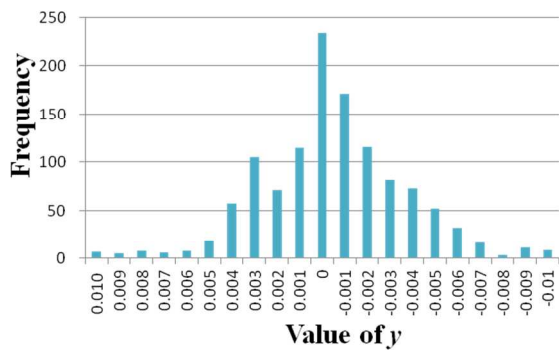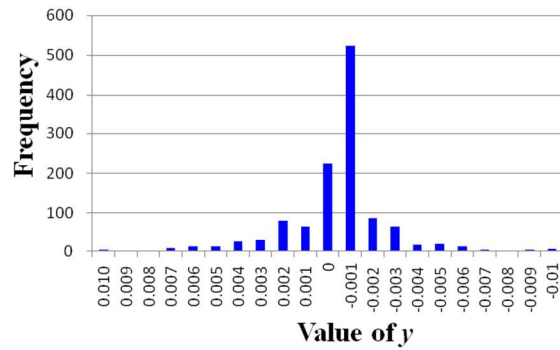**Figure 11.** Reproduction result of measured normal vectors

Figure 12. Probability histogram of the distribution of normal vectors (a) x-components of the measurement value, (b) y-components of the measurement value, (c) x-components of the generated value and (d) y-components of the generated value

Figure 13. Probability histogram of variation (a) x-components and (d) y-components of normal vector

Distribution model of measured normal vectors

Figure 10 shows the distribution of the normal vectors of measured-size mesoscopic facets at intervals of 200 μm. We used combination of measured-size normal vectors to obtain an extended-size of distribution of the normal vectors by inverted the measured-size distribution. We got the extended-size of the normal vector distribution consists of measured-size normal vectors distribution of 4 × 4 to avoid the edge effect of the measured-size distribution as shown in Fig. 10. Figure 11 shows the rendering result for the distribution of measured normal vectors.

Distribution model for generated normal vectors

Each normal vector is resolved into its x-, y-, and z-components. We calculated probability histograms for the measured distribution of the normal vectors for each x- and y-component. Figure 12 (a) and (b) show the measured histograms for each component. In order to generate the distribution, each component is substituted by a random number according to the measured distributions of the normal vectors. The value x_n is calculated by the following equation.

$$x_n = \frac{r - g(i-1)}{g(i) - g(i-1)} \times x_0 + (i-1) \times x_0 \qquad (5)$$

where x_n denotes the random number according to the measured distribution, x_0 denotes x divided by i, i denotes the number of increment, r denotes the random number generated temporarily, $g(i)$ denotes the cumulative distribution function. Equation (5) is applied when $g(i)$ is greater than r. The same calculation is applied to calculate y_n. Figure 12 (c) and (d) show the probability histogram of each x- and y-component generated by this algorithm [9].

In the next step, we consider the relationship between the neighboring facets in the measured the distribution of the normal vectors. Since the normal vectors for the neighboring facets should change smoothly, we calculated the histograms of the variation of each x- and y-component of the measured normal vectors. This is shown in Figure 13 (a) and (b), respectively. The generated normal vector of the mesoscopic facets is based on this variation.

Figure 14 shows a result of the rendering by the generated distribution of the normal vectors. We could reproduce the gloss unevenness by the distribution model of the generated normal vectors. Compared with Fig. 9, in Fig. 14 there is unevenness in the gloss, it was shown that the gloss unevenness is caused by the mesoscopic facets along with in Fig. 11.

Conclusion

We have measured distribution of the normal vectors for the mesoscopic facets. We calculated the probability histogram in consideration of the variation and the normal vectors. We reproduce the gloss unevenness by the Torrance-Sparrow model with the consideration of mesoscopic facets, and found that gloss unevenness is reproduced by this expanded model. As future works, improvement of the accuracy in the generated normal vectors, we discuss evaluation of the gloss unevenness.

References

[1] S. Inoue, N. Tsumura, Relationship between PSF and Gonio-reflectance Distribution of Specular Reflection, Proc. CGIV, pp. 301-306. (2012).

[2] H. Fujiwara, C. Kaga, I. Kano "Measurement of gloss profile," Jour. Japan TAPPI., 10, 44 , pp. 1092-1098. (1990).

[3] S. Inoue, Y. Kojima, M. Takishiro, Measurement Method for PSF of Paper on Specular Reflection Phenomenon, Proc. Pulp and Paper Research, pp. 67-82. (2010).

[4] R. Takano, Y. Suzuki, T. Nakaguchi, K. Miyata, S. Inoue, N. Tsumura, Appearance simulation system of hardcopy based on the measured bidirectional reflectance distribution function, Proc. IMQA, pp. 83-84. (2011).
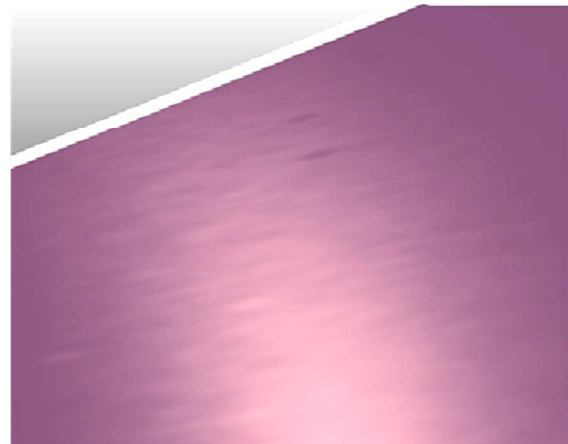
Figure 14. Reproduction result of gloss unevenness

[5] F. R. Clapper and J. A. C. Yule, "The effect of multiple internal reflections on the densities of halftone prints on paper," J. Opt. Soc. Am. 43, pp. 600-603. (1953).

[6] K. E. Torrance and E. M. Sparrow, "Theory or Off-Specular Reflection from Roughened Surfaces," Jour. Opt. Soc. Am., 57, 9, pp. 1105-1112. (1967).

[7] M. Ukishima, Y. Suzuki, N. Tsumura, T. Nakaguchi, M. Makinen, S. Inoue, and J. Parkkinen, Spectral Image Prediction of Color Halftone Prints Based on Neugebauer Modified Spectral Reflection Image Model, Proc. CG IV, pp. 444-451. (2010).

[8] D. B. Judd, "Fresnel reflection of diffusely incident light," Jour. Opt. Soc. Am., 35, 2, pp. 162-162. (1945).

[9] M.T. Boswell, S.D. Gore, G.P. Patil, C. Taillie, "The Art of Computer Generation of Random Variables" Jour. Handbook of Statistics, 9, pp. 661-721. (1993).

[10] ISO 8254-1:2009.

Author Biography

Rui Takano received his B.E. degree from Department of Information & Image Science at Chiba University in 2011. Now, he is a muster course student from the Graduate School of Advanced Integration Science at Chiba University. He is interested in printing, and appearance reproduction. He is a member of the Japan Society of Applied Physics.